Science Signaling
AAAS

www.sciencesignaling.org/cgi/content/full/1/47/ra15/DC1

Supplementary Materials for

γ-Secretase Limits the Inflammatory Response Through the Processing of LRP1

Kai Zurhove, Chikako Nakajima, Joachim Herz, Hans H. Bock, Petra May*

*To whom correspondence should be addressed. E-mail: Petra.May@zfn.uni-freiburg.de

Published 25 November 2008, *Sci. Signal.* **1**, ra15 (2008)
DOI: 10.1126/scisignal.1164263

This PDF file includes:

Supplementary Materials and Methods

Expression plasmids for stable transfection of MEF

Full-length LRP1 [pcDNA3.1-zeo-LRP1 (*1*)], truncated LRP1 mutants LRP1-β-chain (nt 13049-14101 of NM_002332 preceded by a Kozak sequence and the leader peptide) and LRP1-ECD (truncated at nt 13837 of NM_002332 followed by a V5 tag coding sequence), LRP1 ICD (nt 13748-14101 of NM_002332 preceded by a Kozak sequence), and the empty vector (pcDNA3.1, Invitrogen) as control.

Probes for Northern Blotting

Probes used in the analysis of Northern blots were designed based on the following sequences: Cyclophilin (*2*), 25-cholesterol hydroxylase: nt 422-1131 of AF059213; dkk-3: nt114-1165 of AJ243964; C3: nt 4142-4950 of MUSC3B, sfrp-1: nt 361-1192 of U88566, AHR: nt 499-1254 of M94623.

Real-time RT-PCR primers

Cyclophilin forward: 5'- TGG AGA GCA CCA AGA CAG ACA -3', *Cyclophilin* reverse: 5'-TGC CGG AGT CGA CAA TGA T -3'; *GAPDH* forward: 5'-TGT GTC CGT CGT GGA TCT GA-3', *GAPDH* reverse: 5'-CCT GCT TCA CCA CCT TCT TGA T-3'; *Rsad2* forward: 5'- TGT TCC CCT TGA GAA ACT GGG TTA T -3', *Rsad2* reverse 5'- TAT TCC AAA GCA GAA AAG CAT TAG A -3'; *Oas1a* forward: 5'- TGG TCA TCA ATT ATC AGC ATC TTC G -3', *Oas1a* reverse 5'- TCT GTG CAG GTA TTT GGA GAC CTC C -3'; *Tyki* forward 5'- GAA CAT GGT ATT GAA TAT TCT ATC C -3', *Tyki* reverse 5'- CTT GTG ACC AAA TAT GAC TTA ATT C -3'; *Usp18* forward 5'- GAC TTT GGT CAT TAC TGT GCC TAC A -3', *Usp18* reverse 5'- TGT GGT TCC CAT AGG TAC ACT GGA C -3'; *IFN*-γ forward 5'- TCT GAG ACA ATG AAC GCT AC -3', *IFN*-γ reverse 5'- AGG CTT TCA ATG ACT GTG C -3'; *IFN*-β forward 5'-CAT TCG AAG ACT TAC CAG AAA CTT C-3', *IFN*-β reverse 5'-GTA GAT TCA CTA CCA GTC CCA GAG-3'.

Antibodies

The following antibodies were used for the analysis of Western blots: A rabbit polyclonal antibody against a C-terminal epitope of LRP1 (*3*); a rabbit polyclonal antibody against IκBα (Cell Signaling, Frankfurt, Germany; Cat.#9242); a rabbit polyclonal antibody against Hsp90 (StressGen, SPA-846); a rabbit monoclonal antibody against histone 2b (Biomol, EP957Y); a mouse monoclonal antibody against phospho-p65 (Ser^{536}; Cell Signaling Technology; Cat.#3036); a polyclonal rabbit antibody against β-actin (Sigma Aldrich, Cat#A5060); a goat polyclonal antibody against IRF-3 (Santa Cruz, Cat.#sc-15991); and a rabbit polyclonal antibody against phospho-IRF-3 (Ser396; Cell Signaling; Cat.#4961).

Mouse genotyping

Genomic DNA from mouse tissues was prepared and examined by PCR according to standard protocols. The following PCR primers were used for the detection of the recombined and non-recombined LRPlox allele: primer rec1, 5'-GGT GTG ACA TAG AGT TTT AAA GAG G-3'; primer rec2, 5'-GCA AGC TCT CCT GCT CAG ACC TGG A-3'; primer non-rec1, 5'-CAT ACC CTC TTC AAA CCC CTT CCT G-3'; primer non-rec2, 5'-GCA AGC TCT CCT GCT CAG ACC TGG A-3'. For detection of the Cre transgene, the following primers were used:

primer Cre 800, 5'-GCT GCC ACG ACC AAG TGA CAG CAA TG-3'; primer CRE 1200: 5'-GTA GTT ATT CGG ATC ATC AGC TAC AC-3'.

Buffer recipes

RIPA Buffer: 50 mM Tris pH 8.0, 150 mM NaCl, 1 mM EDTA, 1% NP-40, 0.5% (w/v) Na-Deoxycholate, 0.1% (w/v) SDS, 1 pellet Complete Mini EDTA-free Protease inhibitor Cocktail (Roche), Phosphatase Inhibitor Cocktail 1 (Sigma-Aldrich). Buffer A: 10 mM HEPES-KOH, pH 7.8, 1.5 mM $MgCl_2$, 10 mM KCl, 0.5 mM DTT, 0.2 mM PMSF, 1 mM $NaVO_3$. SDS buffer: 10 mM Tris-HCl, pH 6.8, 100 mM NaCl, 1% SDS, 1 mM EDTA. Buffer C: 20 mM HEPES-KOH, pH 7.8, 2.5% (v/v) glycerol, 0.42 M NaCl, 1.5 mM $MgCl_2$, 1 mM EDTA, 0.5 mM DTT, 0.2 mM PMSF, 1 mM $NaVO_4$.

LRP1 sequences used for cloning of GST fusion proteins

NM_002332, nt 13805-14101 (LRP1tail and the NPxY mutants, where the coding sequence for the first, the second, or both NPxY motifs of the LRP1 ICD has been replaced with Ala codons), NM_002332, nt 13805-14008 (LRP1-67).

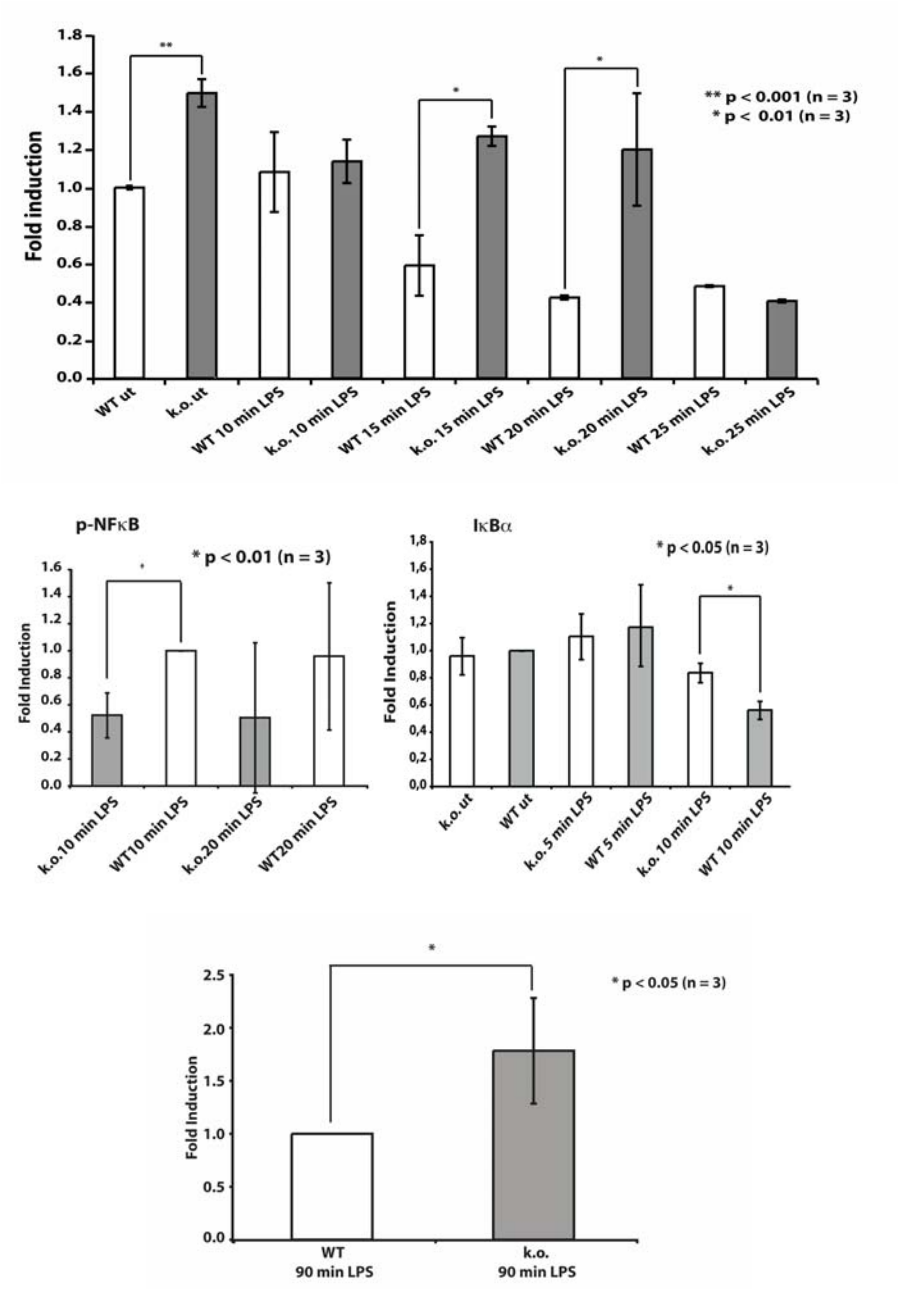

Fig. S1. Quantification of Western blots. Western blots were quantified with the rectangular selection tool of ImageJ software. Data were normalized to the loading control and then the fold induction was calculated by relating normalized expression values to that of the wildtype. The Student's t-test for independent samples was carried out for statistical analysis. Error bars indicate standard deviations. *Top panel*, Quantification of Western blot presented in Fig. 3A; *Middle panel*, Quantification of Western blot presented in Fig. 4A; *Bottom panel*, Quantification of Western blot presented in Fig. 4B.

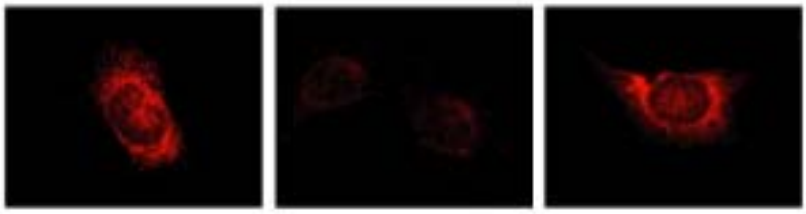

k.o.-LRP1 k.o.-ctrl. k.o.-LRP1-ECD

Fig. S2. Detection of LRP1-ECD in transfected LRP1-deficient fibroblasts. The LRP1 ECD was visualized by immunofluorescence staining with an antibody that binds to LRP1 extracellularly (8G1, Progen).

k.o.-LRP1-ECD

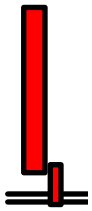

Fig. S3. Schematic representation of the LRP1-ECD mutant transfected into LRP1-deficient fibroblasts.

Fig. S4. Effect of dominant-negative presenilin on the processing of LRP1. Wild-type mouse embryonic fibroblasts were transfected with an expression plasmid encoding a dominant negative mutant of presenilin (dn), in which Asp^{366} of the active site was mutated to Ala, or with the empty control plasmid (c). Presenilin is the enzymatically active component of the γ-secretase complex. Release of the LRP1-ICD is inhibited by the dominant negative mutant and the membrane-bound 25 kD fragment of LRP1 that serves as a substrate of γ-secretase accumulates, as is demonstrated in membrane preparations from the transfected cells.

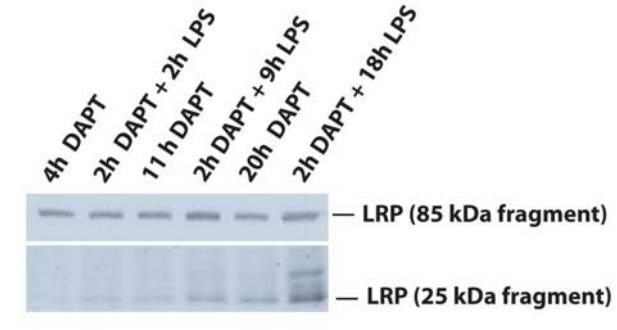

Fig. S5. Time course of DAPT treatment. A time course experiment was conducted similarly to the experiment presented in Fig. 2A, in which DAPT (10 μM)-pretreated wild-type macrophages were stimulated with LPS (1 μg/ml) for increasing lengths of time. This treatment led to the progressive accumulation of the membrane-bound, 25 kD LRP1 fragment.

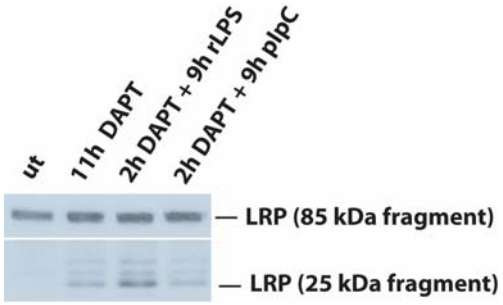

Fig. S6. Effect of purified rLPS on the processing of LRP1. The experiment represented in Fig. 2A was repeated with highly purified rLPS generously provided by M. Freudenberg and C. Galanos (MPI for Immunobiology, Freiburg, Germany). rLPS had essentially the same stimulatory effect on LRP1 processing that had been observed with the commercial LPS preparation. Another activator of the innate immune system, pIpC, did not increase proteolytic processing of LRP1.

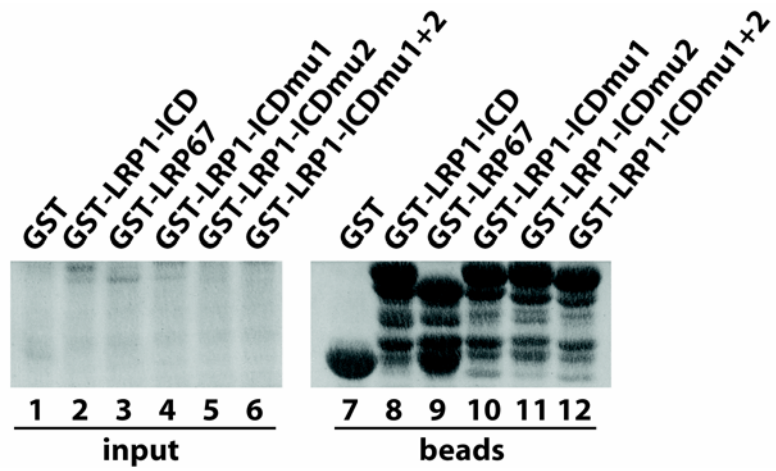

Fig. S7. Analysis of fusion proteins. Ponceau red staining confirms equal input of fusion proteins into the pulldown experiment presented in Fig. 3H.

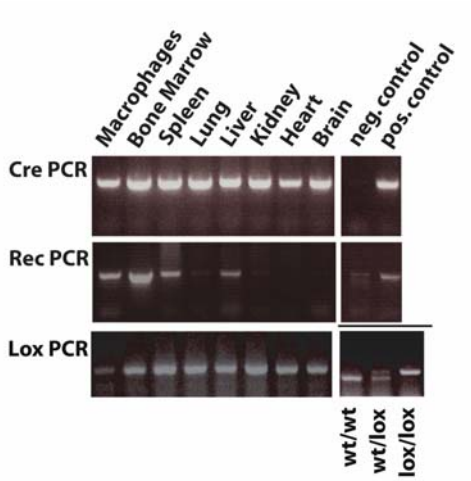
Macrophages
Bone Marrow
Spleen
Lung
Liver
Kidney
Heart
Brain
neg. control
pos. control
Cre PCR
Rec PCR
Lox PCR
wt/wt
wt/lox
lox/lox

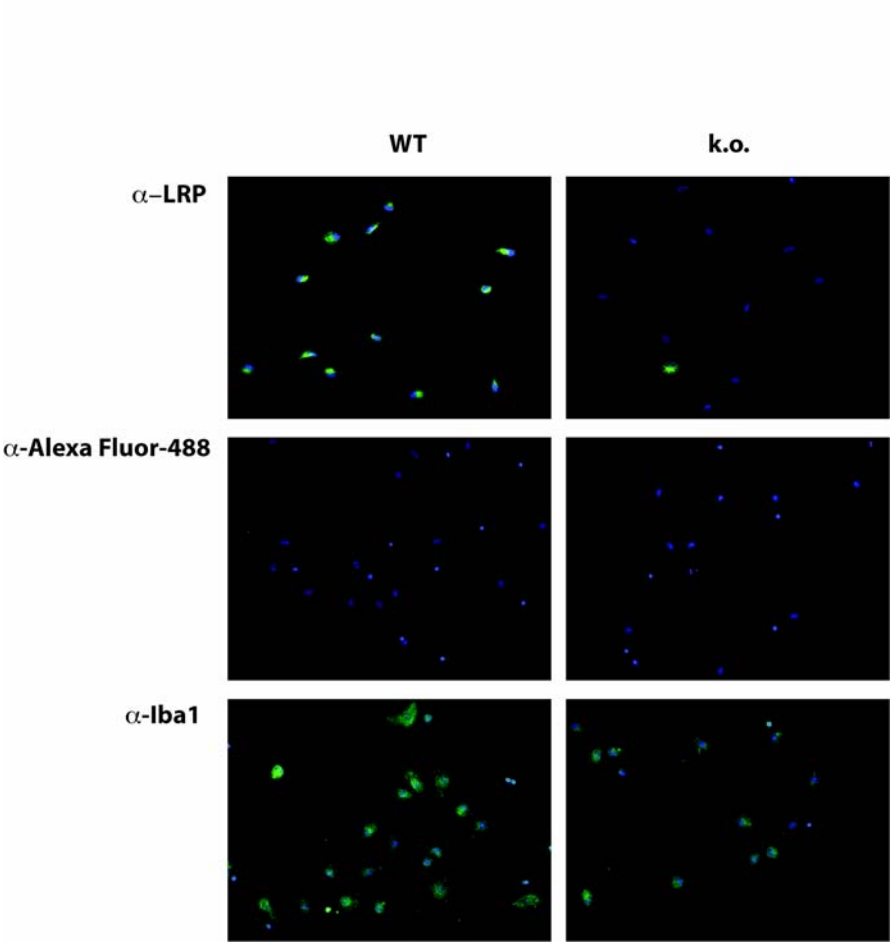
WT
k.o.
α–LRP
α-Alexa Fluor-488
α-Iba1

Fig. S8. Analysis of macrophages from wild-type and conditional *LRP1*$^{-/-}$ mice. *Top panel*, Genomic DNA was prepared from peritoneal macrophages and different tissues of conditional *LRP*$^{-/-}$ (LysCre;LRP1$^{lox/lox}$) mice and then analyzed by PCR with primers that detect the presence of the Cre transgene, primers that bind to the non-recombined floxed *LRP1* allele (lox), and primers specific for the recombined allele (rec). Recombination can be detected in macrophages and in all tissues that contain a significant amount of myeloid cells. The lox PCR shows that even in macrophages, some non-recombined DNA persists, indicating incomplete efficiency of recombination. *Bottom panels*, Macrophage preparations from LysCre;LRP1$^{lox/lox}$ mice and from LRP1$^{lox/lox}$ controls were analyzed by immunocytochemistry. Samples were stained with an antibody against LRP1 or with an antibody against the macrophage marker Iba1 and counterstained with DAPI (blue). In macrophages from the Cre transgenic mice LRP1 was lost in almost all cells. Some cells, however, retained LRP1 as would be expected with the incomplete recombination seen above. Alexa-Fluor 488: Control staining with the secondary antibody alone.

Supplementary Table 1. Effects of LRP1 deficiency on target gene expression. Gene expression was compared between wild-type and LRP1-deficient fibroblasts and the tranfected cell lines by microarray analysis. A subset of genes whose expression was increased in the absence of LRP1 was decreased by transfection of LRP1 or the LRP1-β-chain, but not by the LRP1-ECD. SLR, Signal Log Ratio; I, increase; NC, no change; MI, marginal increase; D, decrease. The change is expressed as logarithm to the base 2.

Gene Title and Symbol	k.o. vs wt		k.o.-vector vs wt		k.o.-LRP1 vs wt		k.o.-LRP1.□chain vs wt		k.o.-LRP1-ECD vs wt	
	SLR	Change	SLR	Change	SLR	Change	SLR	Change	SLR	Change
2'-5' oligoadenylate synthetase 1A, Oas1a	2.2	I	4.3	I	0.9	NC	-0.6	NC	3.4	I
thymidylate kinase family LPS-inducible member, Tyki	1.1	I	3.4	I	-0.7	NC	-0.4	NC	1.4	I
ubiquitin specific protease 18, Usp18	1.8	I	5	I	0.7	MI	-1.1	D	2.7	I
radical S-adenosyl methionine domain containing 2, Rsad2	1.5	I	4.3	I	-0.4	NC	0.2	NC	2.4	I
radical S-adenosyl methionine domain containing 2, Rsad2	1.7	I	4.6	I	0.2	NC	-0.3	NC	3.2	I
5-oxoprolinase (ATP-hydrolysing), Oplah	1.3	I	1.6	I	-1.7	NC	-0.2	NC	1.1	I
interleukin 6 receptor, alpha, Il6ra	1	I	1	I	0.8	NC	0.3	NC	1.1	I

Supplementary Table 2. Differential gene expression in wild-type and LRP1-deficient fibroblasts. RNA samples from wild-type and LRP1-deficient fibroblasts were analyzsed by hybridization to microarray chips. Differentially expressed genes included genes related to lipid metabolism, membrane trafficking, signal transduction, and transcriptional regulation. The fold induction in expression in LRP1-deficient cells is given in parentheses.

Transcription factors and signaling-related molecules:
Paired-like homeodomain transcriptionfactor 2 (0.05)
Sine oculis-related homeobox 2 (0.14)
Paired box gene 6 (0.25)
SRY-box containing gene 2 (22.6)

Secreted frizzled-related protein 1 (0.07)
Dickkopf 3 (0.13)
Wnt 10a (2.8)

Similar to receptor-type PTP zeta (0.04)
Pleiotrophin (0.25)

Eps8 (3.0)
Epiregulin (3.0)
HB-EGF (3.0)

Latent TGF BP-1 (3.7)
Schnurri-2 (3.7)

G_{1}□ (0.07)
CEBP/delta (3.7)
Arylhydrocarbon Receptor (4.0)
Interferon-activated gene 204 (4.0)
Interferon-activated gene 202 (4.2)
Groucho-related protein 1 (4.3)
Preproenkephalin (16.0)
Autotaxin (55.7)

Membrane Trafficking:
Annexin 8 (32.0)
Syntaxin 3a (3.0)

Lipid/LipoproteinReceptor Metabolism:
Keratinocyte lipid binding protein (0.33)
Cellular retinoic acid binding protein (3.2)
25-Cholesterol-Hydroxylase (7.0)
NGAL (8.5)

Others

Thy-1.2 glycoprotein gene (0.03)
Thrombomodulin (0.17)
Peg1/MEST (0.18)
Osf-2 (0.19)
Cystein rich intestinal protein (0.19)
Gro1 (3.0)
Connexin 43 (3.0)
C3 (5.4)
Osteopontin (12.1)

References

1. P. G. Ulery, J. Beers, I. Mikhailenko, R. E. Tanzi, G. W. Rebeck, B. T. Hyman, D. K. Strickland, Modulation of beta-amyloid precursor protein processing by the low density lipoprotein receptor-related protein (LRP). Evidence that LRP contributes to the pathogenesis of Alzheimer's disease. *J. Biol. Chem.* **275**, 7410-7415 (2000).
2. E. G. Lund, C. Xie, T. Kotti, S. D. Turley, J. M. Dietschy, D. W. Russell, Knockout of the cholesterol 24-hydroxylase gene in mice reveals a brain-specific mechanism of cholesterol turnover. *J. Biol. Chem.* **278**, 22980-22988 (2003).
3. J. Herz, U. Hamann, S. Rogne, O. Myklebost, H. Gausepohl, K. K. Stanley, Surface location and high affinity for calcium of a 500-kd liver membrane protein closely related to the LDL-receptor suggest a physiological role as lipoprotein receptor. *EMBO J.* **7**, 4119-4127 (1988).